RSC Advances

PAPER

View Article Online
View Journal | View Issue

Cite this: *RSC Adv.*, 2024, **14**, 18296

Ursolic acid inhibits NF-κB signaling and attenuates MMP-9/TIMP-1 in progressive osteoarthritis: a network pharmacology-based analysis†

Eman Maher Zahran,[a]* Soad A. Mohamad,[b] Mohamed M. Elsayed,[c] Mohamed Hisham,[d] Sherif A. Maher,[e] Usama Ramadan Abdelmohsen,[af] Mahmoud Elrehany,[g] Samar Yehia Desoukey[f] and Mohamed Salah Kamel[f]

Osteoarthritis (OA) is a degenerative joint disease, characterized by infiltration of monocytes into the synovial joint which promotes inflammation, stiffness, joint swelling, cartilage degradation and further bone destruction. The leaves of *Ocimum forskolei* have been used for inflammation-related disease management in traditional medicine. Additionally, the downregulation of NF-κB and the MMP/TIMP-1 ratio has been shown to protect against OA. The LC-HR-MS metabolic analysis of *Ocimum* yielded 19 putative compounds, among which ursolic acid (UA) was detected. Ursolic acid possesses significant anti-inflammatory effects and has been reported to downregulate oxidative stress and inflammatory biomarkers. It was tested on rats in a model of intra-articular carrageenan injection to investigate its efficacy on osteoarthritis progression. The UA emulgel exerted chondroprotective, analgesic and local anaesthetic efficacies confirmed *via* histopathological investigation and radiographical imaging. A network pharmacology followed by molecular docking highlighted TNF-α, TGF-β and NF-κB as the top filtered genes. Quantitative real-time PCR analysis showed that UA significantly attenuated serum levels of *TNF-α*, *IL-1β*, *NF-κB*, *MMP-9/TIMP-1* and elevated levels of *TGF-β*. Taken together, these results suggest that UA could serve as a functional food-derived phytochemical with a multi-targeted efficacy on progression of OA, regulating the immune and inflammatory responses, particularly, attenuating chondrocytes degeneration *via* suppression of *NF-κB* and *MMP-9/TIMP-1*. Accordingly, UA might be a promising alternative to conventional therapy for safe, easily applicable and effective management of OA.

Received 14th April 2024
Accepted 30th May 2024

DOI: 10.1039/d4ra02780a

rsc.li/rsc-advances

Introduction

Osteoarthritis (OA) is the most common articular degenerative disease characterized by cartilage degradation, synovitis, collagen loss, subchondral bone damage and sometimes osteophyte formation, resulting in joint stiffness, swelling and pain.[1] The WHO identified OA as the fastest growing major public health problem and the second prominent cause of global disability, especially in geriatrics, which reduces patients' quality of life and results in serious social and economic burdens.[2] Based on population-based healthcare data from England and Sweden in 2014, 13% of the elderly were diagnosed with OA. Approximately 25% of the population over 55 reports at least one knee pain attack every year, which strongly reflects the potential of OA.[3] Yet the etiology is not fully assumed, it includes various biochemical and mechanical factors that trigger pro-inflammatory cytokines and chondrolytic enzymes that disrupt the equilibrium between physiologic synthesis and degradation of articular cartilage.[4]

The traditional perception of OA as a mechanical 'wear and tear' condition that eventually leads to cartilage degeneration has been developed by the fact that inflammation is central to OA progression in all stages. When chondrocytes undergo inflammation, the NF-κB signalling activates the matrix metalloproteinases (MMPs), which in turn catalyzes the breakdown of extracellular matrix (ECM) and cartilage. Accordingly, a cross talk might be established between inflammatory markers triggered by NF-κB and 2 main cell types including: immune cells

[a]*Department of Pharmacognosy, Faculty of Pharmacy, Deraya University, Universities Zone, New Minia City, 61111, Egypt. E-mail: emanzahran84@yahoo.com; eman.maher@deraya.edu.eg*

[b]*Department of Pharmaceutics and Clinical Pharmacy, Faculty of Pharmacy, Deraya University, Universities Zone, New Minia City, 61111, Egypt*

[c]*Faculty of Pharmacy, Deraya University, Universities Zone, New Minia City, 61111, Egypt*

[d]*Department of Pharmaceutical Chemistry, Faculty of Pharmacy, Deraya University, Universities Zone, New Minia City, 61111, Egypt*

[e]*Department of Biochemistry, Faculty of Pharmacy, New Valley University, New Valley, Elkharga 71511, Egypt*

[f]*Department of Pharmacognosy, Faculty of Pharmacy, Minia University, 61519 Minia, Egypt*

[g]*Department of Biochemistry, Faculty of Pharmacy, Deraya University, Universities Zone, New Minia City, 61111, Egypt*

† Electronic supplementary information (ESI) available. See DOI: https://doi.org/10.1039/d4ra02780a

and joint resident cells. The T-helper cells produce pro-inflammatory cytokines which stimulate resident cells (fibroblasts, osteoblasts, osteoclasts and chondrocytes) to secret additional pro-inflammatory factors.[5] These factors create the main joint pathological events as: synovitis, cartilage damage, pannus and osteophyte formation.[6] Both the immune and joint-resident cells provide feedback on chondrocytes and stimulate production of more pro-inflammatory mediators, functional deregulation of the chondrocytes and subsequent damage.[7]

Actually, a wide range of cytokines is implicated in activating synovial tissue and mediating cartilage breakdown in OA, where blocking a single pro-inflammatory mediator failed to result in symptomatic improvement. Currently, there is no effective pharmacotherapy available to restore the damaged articular cartilage, and conventional therapies are still restricted to analgesics which cause major toxicity risks associated with renal failure and GIT problems, nutrients as glucosamine, physical therapy or even surgical intervention in severe cases.[3] Such therapeutic limitations have sparked the search for alternative treatments such as herbal medicines, especially those from edible sources, or their constituents that might add benefit for such emerging cases.[8] To date, studies have shown that many herbal extracts provide relief of inflammation symptoms, probably by interference with the proinflammatory cascade, however, concerns regarding the therapeutic relevance, exact mechanisms or applicability of most of them has not yet been reached.[9,10] *Ocimum forskolei* is a lamiaceous aromatic plant with antioxidant, anti-inflammatory, gastroprotective, anti-epileptic, local anaesthetic, antimicrobial and antiproliferative efficacies.[11–13] Ursolic acid (UA) is an ursane-type triterpene phytoconstituent of *O. forskolei* and many other herbs and peels of fruits, which attains potent antioxidant, anti-inflammatory, gastroprotective and cytotoxic efficacies.[14]

Since the development of systems biology and bioinformatics, modern technology has entered the aria of omics and huge data that researchers have used to explore the diseases/drugs correlation.[15] Network pharmacology explains the relationship between the body and the drugs from the perspective of restoring the balance of biological networks as well as building a "drug-targeted disease" network.[16] Hence, the network pharmacology explores the mechanism of UA on OA at the molecular level, elucidate the specific targets and signalling pathways, and creates new strategies for therapeutic development and clinical applications of UA.

Accordingly, the main objective of the present study is to evaluate the chondroprotective effects of UA, against early-stage progression of OA using the carrageenan intra-articular (CIA)-induced model in rats, supported by mRNA gene expression as well as network pharmacology and docking analysis to assess the molecular mechanisms underlying UA effects.

Materials and methods

General experimental procedure

The leaves of *Ocimum forskolei* were collected in September 2022 from ElZohria Garden, Cairo, Egypt. The specimens were kindly identified according to standard taxonomic keys, and a voucher specimen (PH-11-2022) was deposited at the Department of Pharmacognosy, Faculty of Pharmacy, Deraya University, Egypt. Extraction and fractionation into 4 different fractions: *n*-hexane, dichloromethane and ethyl acetate and aqueous fractions was performed, where the *n*-hexane fraction was further subjected to Liquid Chromatography-High Resolution-Mass spectrometry (LC-HR-Ms analysis),[17] see details of the experiment in the supplementary section. The compounds were dereplicated and identified using the Dictionary of Natural Products (DNP) database and comparison with data reported in literature.[17]

(Table S1, Fig. S1 & S2†). Then, the *n*-hexane fraction was subjected to Vacuum Liquid Chromatography (VLC) followed by column chromatography and yielded ursolic acid which was identified *via* ^{1}H-NMR chromatography techniques (see ESI data for details, Fig. S3†).

Formulation, characterization and *in vitro* permeability investigation of UA-emulgel

Formulation of ursolic acid-loaded emulgel (UA-emulgel). UA acid was formulated into emulgel in 3 different formulations: UAE1, UAE2 and UAE3. (For more details see ESI data, Tables S2 & S3, Fig. S4 & S5†).

Characterization of UA-emulgel

The 3 formulations were organoleptically and physically compared, then characterized by viscosity, drug content, pH, swelling and presence of any foreign particles.[18] The formulation (UAE2) was selected for further studies based on the best characterization features.

The drug content, bioadhesion force and permeability were measured, the centrifugation test was used to check the stability of emulgel which was visualized and checked for morphology *via* scanning electron microscope[19] (Table S4, ESI data†).

Biological studies

Ethics statement

This study fully adheres to the WHO's international Guiding Principles for biomedical Research Involving Animals.[20] The study has been reviewed and approved by Animal Care and Use Committee of Deraya University under the approval number 15/5/2022.

Intra-articular carrageenan-induced acute monoarthritis model in rats

Adult male Albino Wistar rats (100–150 g) were used for the study, acclimatized and subjected to the skin irritation test of the emulgel.[21] A standardized rat animal model of acute monoarthritis was constructed to assess the degree of resultant joint inflammation *via* intra-articular (IA) injection of carrageenan in one knee of each animal, where the other knee is used as a control.[22]

Four groups of animals were designed with 6 animals each ($n = 6$).[23]

Group **I** (positive control group, induction without treatment). The treatment groups were divided into 3 subgroups: group **II** (plain emulgel group), group **III** (UA-emulgel treated group) and group **IV** (The standard, Algason® treated group). Algason® is a massage cream composed of (camphor oil 1.4 g + menthol 2.5 g + diethylamine salicylate 15 g) and is widely used in rheumatic pain conditions. All animals were anaesthetized, to reduce pain, with thiopental sodium (50 mg kg^{-1}, i.p.), followed by IA injection in the left knee joint with 0.1 mL of 3% carrageenan dissolved in 0.9% NaCl. The inflammation is confirmed by the presence of swelling, erythema and hyperalgesia.[23]

Anti-inflammatory assessment

A definite amount (0.2 g) of each preparation was applied to the corresponding group to the left knee joint and massaged gently for 2 min, while the right knee was left as a control. The knee joints were measured before the IA injection as a baseline and at 30 min, 1, 2, 4, 6 and 8 h after the IA injection on the same day, at the distance between the lateral and medial collateral ligament region, where the percentage oedema inhibition was calculated (Table S5†).

Being an acute mono-arthritis model, the radiography was employed to determine the real degree of tissue swelling and its degree of extension either upward or downward the knee joint.[1] Additionally, tissue samples from all groups were employed for H & E histopathological study.[24]

Analgesic assessment

The paw withdrawal model of hyperalgesia was used for analgesic assessment of the tested groups (**I–IV**), where the maximal possible analgesia was measured[25] (see ESI data for details of the experiment, results are reported in Table S6†).

Local anaesthetic assessment

Under thiopental anaesthesia, the left sciatic nerve was isolated under aseptic surgical conditions *via* the biceps femoris blunt dissection, without damage to the perineurium (Fig. S6†). The nerve conduction was checked *via* applying weak sudden electric shocks of 1 ± 0.2 mA and observing the leg reflexes (local muscular twitches). Then, a number of other 24 animals (4 groups of 6 animals, each)were sub grouped into: group **I** (positive control group, induction without treatment). The treatment groups were divided into 3 subgroups: group **II** (plain emulgel group), group **III** (UA-emulgel treated group) and group **IV** (The standard, Lidocaine® treated group). Treatments were applied directly to the sciatic nerve, then the electric shocks were applied at 1 m, 2 m, 3 m, 15 m, 30 m, 1 h, 2 h and up to 3 h. With both onset and latency of leg reflexes recorded[26] (Table S7, Fig. S6†).

Network pharmacology

The GeneCards and Comparative Toxicogenomics Database (CTD) were used to establish a database for osteoarthritis targets, while the ursolic acid-related targets were collected *via* searching within the Traditional Chinese Medicine Systems Pharmacology, Analysis Platform (TCMSP) and BATMAN-TCM platform databases.[27] The interactive network map of "ingredient-target" was built with Cytoscape software (Version 3.10.0) (USA). The related protein interaction relationship was analysed following construction of the protein–protein interaction (PPI) network with the STRING database.[28] (ESI data†).

Molecular docking

The Maestro and the Glide algorithm, both of which are included in the Schrodinger Small Drug Discovery Suite 2021-2 were employed, besides the protein preparation wizard, the Schrodinger's graphical user interface, the tool's receptor grid generation, the glide tool, the pose organizer tools as well as Maestro.[29] The X-ray crystallographic structures of targets were obtained from the Protein Data Bank as (PDB: **2AZ5**, ligand ID: **307**) for TNF-α, (PDB: 1VJY, ligand ID: 460) for TGF-βR1,[30] (PDB: 1SVC) for NF-κB, (PDB: 6AGF) for Voltage Gated Sodium Channel, and (PDB: 4XCT) for MMP-9 (ref. 31) (Tables S8 & S9, see ESI data†).

Total RNA extraction and real-time qRT-PCR

About 100 mg of the inflamed knee tissues from all groups were homogenized for extraction of total RNA in 1 mL TRIzol reagent and the RevertAid H Minus First Strand cDNA synthesis kit following the manufacturer's instructions and using GAPDH (glyceraldehyde-3-phosphate dehydrogenase) as a reference housekeeping gene to determine the relative expression of *TNF-α*, *IL-1β*, *TGF-β*, *IL-6*, *NF-κB*, *MMP-9*, *TiMP-1* and *COX-II*.[32,33] The primer sequences are illustrated in Table S10.†

Statistical analysis

The data was manipulated using the statistical package Graph Pad prism version 7 software. Statistical differences between groups were calculated using the chi-square test for qualitative variables, independent sample *T*-test, and 2 way-ANOVA (analysis of variance) with *post hoc* Bonferroni test for quantitative normally distributed variables. *P*-Values less than or equal to 0.05 were considered statistically significant, while those more than 0.05 were considered non-statistically significant.

Results

Metabolic profiling and isolation of ursolic acid

LC-MS investigation using HR-LC-MS for the *n*-hexane fraction of *Ocimum forskolei* leaves extract revealed the presence of various classes of metabolites shown in (Fig. S1, Table S1†). Annotation of the compounds was carried out depending on HR-ESI-MS and comparing with the data reported in literature. The compounds were identified as 4-hexenoic acid (**1**),[34] fumaric acid (**2**),[35] dihydroxybenzoic acid (**3**),[36] eugenol (**4**),[37] vanillic acid (**5**),[38] ligustilidiol (**6**),[39] 12-hydroxy jasmonic acid (**7**),[40] sacidumol A (**8**),[41] Nigellicine (**9**),[42] 2-hydroxy-9,12,15-octadecatrienoic acid (**10**),[43] sanguinone A (**11**),[44] synparvolide C (**12**),[45] aegyptinone A (**13**),[46] scillascillin (**14**),[47] sahandone (**15**),[48] 5-*O*-caffeoylshikimic acid (**16**),[49] 5-*O*-*p*-coumaroylquinic acid (**17**),[50]

3-(3,4-dihydroxyphenyl)-2-hydroxypropanoic acid (**18**)[51] and ursolic acid (**19**)[52] (Fig. 1).

The obtained ursolic acid (UA) was identified *via* ^{1}H-NMR spectroscopic analysis (Fig. S3†).

Formulation and characterization of the proper UA-emulgel

According to results shown in Tables S3 & S4,† the formulation UA-E2 was selected for biological study due to stability and high swelling index (Fig. S5†). Formulation UA-E2 attained a high content of OH-groups in chitosan, glycerol as well as lecithin, besides the role of the acidic medium which increases the swelling ability of chitosan. Accordingly, it attains the highest bioadhesion forces, the highest viscosity (301 Pa) as well as the highest drug content (90%), all of which are proper for better topical formulation.

Investigating the SEM results (Fig. 2a and b), the UA-E2 showed well-defined spherical globules with smooth surfaces. The formed O/W emulsion showed a relatively large particle size of 3–5 μ which is preferred for increasing settling time of the drug on the target place. Moreover, the formulation attained a zeta potential value of +55 ± 10 mV that ascertains the highest product stability as it generates a solid interface between oil and water.

Investigating the release profiles of both UA and UA-E2 (Fig. 2c), the results showed a great enhancement of the drug release after incorporation in the prepared emulgel ($F_2 < 50$). The % amount of UA released after 30 min (a burst release) was 12.3% ± 0.16 for UA compared to 53.5% ± 3 of UA-E2, and 43.5% ± 2 for

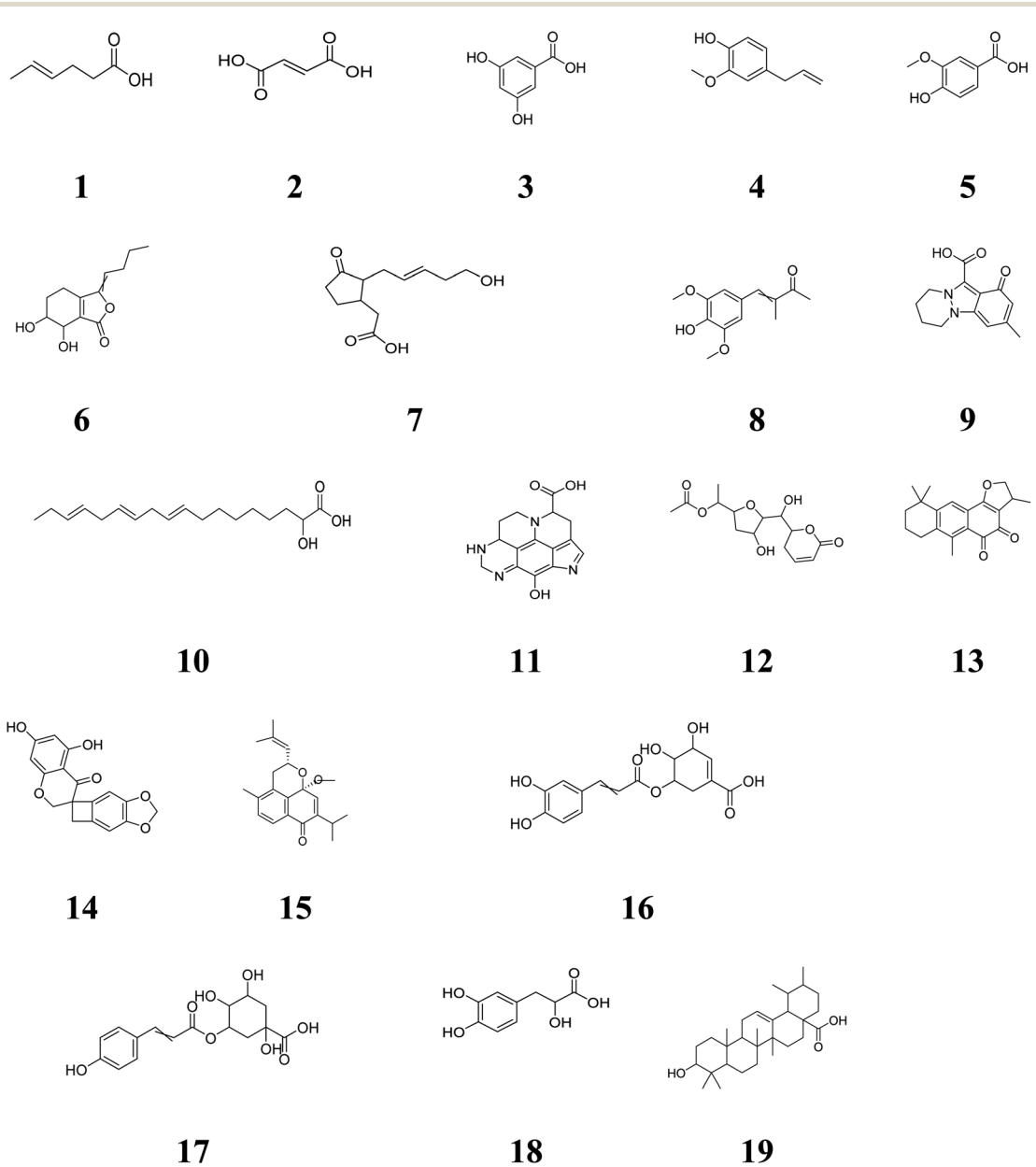

Fig. 1 Annotated compounds from HR-MS spectral data of *n*-hexane fraction of *Ocimum forskolei*.

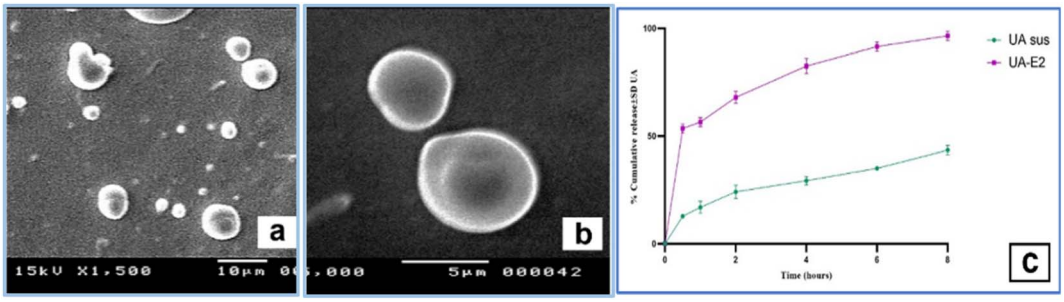

Fig. 2 (a & b) SEM of O/W emulsion of UA-E2, (c) percent cumulative release of UA from suspension and UA-E2. Each value represents the mean ± SD ($N = 6$). Statistical analysis were done by one-way ANOVA followed by the Student's T-test (*$P < 0.05$).

UA compared to 93% ± 0.1 for UA-E2 after 8 h, respectively. These data were well fitted with the Baker–Lonsdale model that had the highest correlation coefficient ($r = 0.99$).

Biological study

The CIA-induced knee edema model in rats triggered a unilateral aseptic inflammation including: knee joint swelling, increased intra-articular pressure, knee hyperthermia and edema. The inflammation severity reached the maximum on day 1 and 2 which stimulated the early stage of OA. On day 3, anti-inflammation, analgesia and local anaesthesia were assessed 60 min after the application of first dose of UA-emulgel. Algason® application couldn't reduce inflammation after a single-dose administration but UA-emulgel completely reversed the mechanical hypersensitivity at the same time and during the time of the experiment (Fig. 3a and b).

Investigating the results expressed in table S5,† UA-emulgel attained the highest % inhibition of oedema (23.80%), 30 min post application and till the end of the experiment at 8 h (60.65%), compared to Algason® cream at the same times with 4.75% and 48.4%, respectively.

Investigating X-ray results, a soft tissue swelling around the joint expressed in an enlargement in the knee transverse diameter was clearly observed in the carrageenan group, while the UA-emulgel group showed a reduced knee diameter, a relatively clear area around the joints and absence of inflammatory spread. The Algason® group showed a moderate degree of soft tissue swelling around the joint extending down the hind limb indicating a tissue inflammation (Fig. 4a–c).

The H & E sections from the inflamed tissues around the knee joints of normal control rats showed normal architecture of the skin consisting of epidermis, dermis, hypodermis, hair follicles and glandula sebacea (Fig. 4d and e). The inflamed tissues showed an increase in the thickness of the sub-epithelial layer, a congestion and a distinct oedema that diffuses the dermal tissue. Additionally, a mononuclear inflammatory cell infiltration has also appeared in the interstitial tissue of the sub dermis, admixed with a large number of neutrophils accompanied with marked hyalinization and blood vessel congestion (Fig. 4f and g). Sections from Algason® group revealed severe oedema with compressed dermis, cell infiltration and congestion of blood vessels (Fig. 4h), while those from the UA group showed a more thickened dermis, less oedema and cellular infiltration, as well as absence of congested blood vessels (Fig. 4i).

The results of the analgesic assessment showed that UA-emulgel exhibited a significant analgesic activity with a short onset of 15 min and latency to leg withdrawal of 5 s. Which tended to endure over the next 10–60 min (Table S7,† Fig. 5a and b), compared to Lidocaine ® which gave a similar onset but a shorter duration (Fig. 5c).

Regarding the local anaesthetic assessment, it is observed that the application of an electric current (3 mA) to an exposed rat sciatic nerve produces strong and repeated leg reflexes which

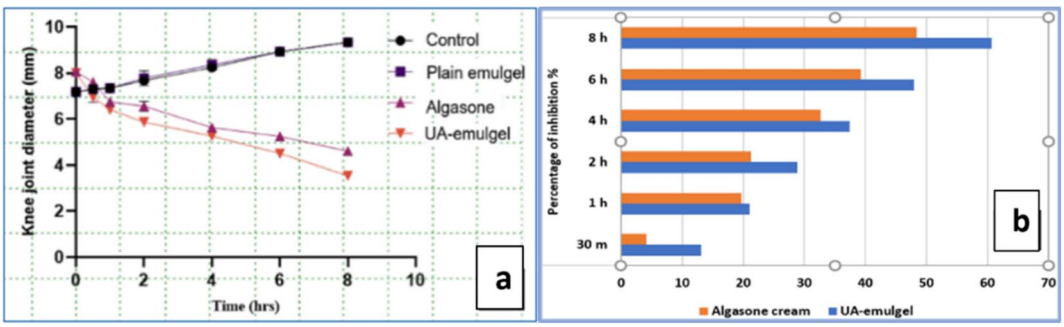

Fig. 3 (a) Results of anti-inflammatory activity, (b) inhibition % of oedema, bars represent mean ± SD ($N = 6$). Statistical analysis were done by one-way ANOVA followed by the Student's T-test (*$P < 0.05$).

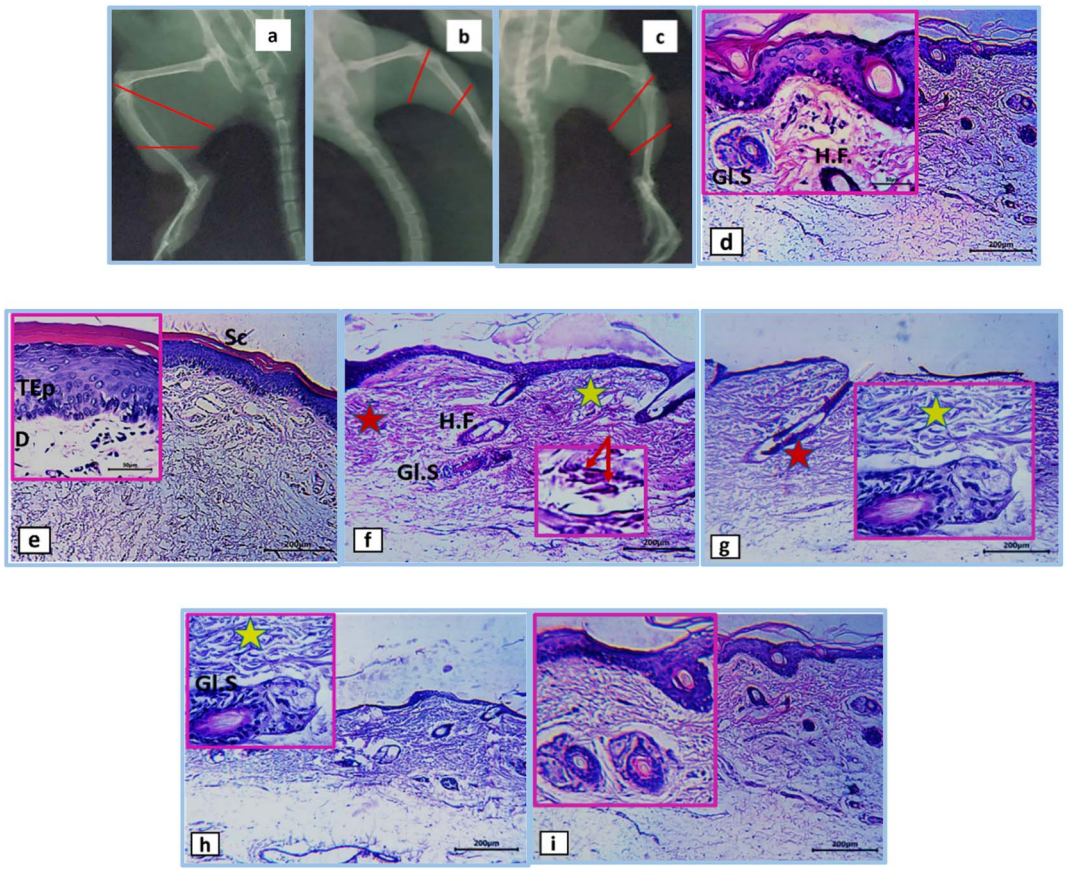

Fig. 4 [X-ray radiography of (a) untreated, (b) UA-emulgel, (c) Algason group], [H & E images of (d) & (e) normal group, (f) & (g) non-treated group, (h) Algason group and (i) UA-emulgel group]. Sc; stratum corneum, TEp; thickened epidermis, D; dermis, Gl.S; glandula sebacea, H.F.; hair follicle; yellow asterisks; cell infiltration, red asterisks; tissue necrosis, red arrows; congested blood vessels.

lasts till the end of the experiment (Fig. S6†). The results (Table S8†) revealed a strong local anaesthetic action of UA-emulgel which started immediately 1 min. Post-application and gave increased latencies till the end of the experiment (3 h). On the other hand, the reference, Lidocaine®, gave the same onset of anaesthetic action, but decreased latencies than UA-emulgel with a loss of efficacy after 1 h (Fig. 5c).

Searching the 2 herbal databases, TCM Systems Pharmacology and BATMAN-TCM platform for potential target proteins corresponding to UA, and after removing duplicates, a total of 124 target proteins were obtained and converted into their gene names using the UniProt database. After querying the GeneCard and databases, limited to entries with an interference score greater than or equal to 35, a comprehensive list of 276 potential therapeutic targets for osteoarthritis was acquired. Upon creating the Venn diagram to compare the targets regulated by ursolic acid and the potential targets for osteoarthritis, it revealed a total of 27 common intersection targets. These targets hold promise as potential therapeutic targets for ursolic acid in the treatment of osteoarthritis as shown in Fig. 6a.

The set of 27 intersected target genes were entered into the STRING database for PPI analyses, where the PPI network diagram was generated and visualized using the Cytoscape 3.10.0. Using Cytoscape's network analyzer, a protein interaction network was constructed consisting of 23 connected nodes and 167 edges, where the average node connectivity was 14.52. To visualize the network, the "yFiles circular layout" tool was employed within the Cytoscape software, and the nodes' sizes were adjusted according to their degree of connectivity, as depicted in Fig. 6b. Utilizing the Cytohubba analysis tool, the top 10 filtered hub genes based on the degree of connectivity, identified as: IL6, TNF, IL1B, VEGFA, CCND1, MMP9, CASP3, STAT3, PTGS2 and BCL2L1 (Fig. 6c). The topological parameters such as node degree, betweenness, and closeness for each protein as well as bone tissue expression score are summarized in Table 1.

Docking results

Based on PPI network results, 5 targets were filtered out of the resultant top 10 targets which are strongly relevant to the NF-κB pathway. The binding modes and the resultant energy scores of UA binding with TNF-α, TGF-β and NF-κB proteins were calculated *via* the computational program Schrodinger Small Drug Discovery Suite 2021-2 and summarized in Table S8.†

The co-crystallized ligand was re-docked with the active pocket of TNF-α, resulting in a glide score (g-score) of -4.68 kcal mol^{-1}, through an arene–cation interaction between the nitrogen of the amino group surrounding the indole

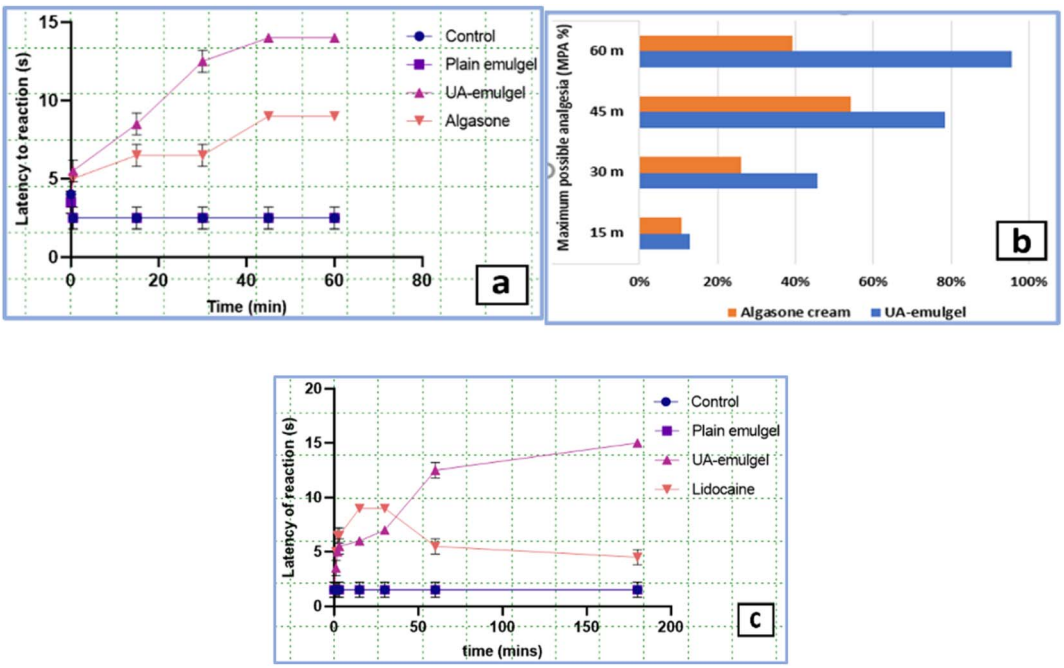

Fig. 5 (a) Results of analgesic activity, (b) maximum possible analgesia, (c) results of local anaesthetic activity. Each value represents the mean ± SD ($N = 6$). Statistical analysis were done by one-way ANOVA followed by the Student's T-test (*$P < 0.05$). Network pharmacology-based analysis.

scaffold and the critical amino acid Tyr119, it was well-attached in the TNF-α binding pocket (Fig. 7a and b). When UA was docked in the active site of TNF-α, the OH group established a hydrogen bond with Leu120 amino acid residue (2.63 Å), resulting in g-score of = −2.85 kcal mol^{-1} (Fig. 7c and d). Regarding docking with TGF-R1 UA was docked with ligand **460** had a g-score of −8.5 kcal mol^{-1} formed by two H-bonding interactions: naphthyridine nitrogen atom with His 283 (2.38 Å) and the pyrazolidine-H with Asp 351 (1.94 Å), as well as a salt bridge between the nitrogen cation of the pyridine moiety with carboxylate anion of Glu 245 (4.18 Å) (Fig. 7e and f).

Interestingly, UA showed an excellent g-score (−3.04 kcal mol^{-1}), with three hydrogen bond interactions: two correspond to both hydroxyl-O (2.66 Å) and hydroxyl-H (2.60 Å) with Glu 228 and the second of carbonyl-O with Lys 342 (1.93 Å). Moreover, a salt bridge was also formed between UA carboxylate anion with Lys 342 (3.64 Å) (Fig. 7g and h). In addition, UA docked in NF-κB active site resulted in a good glide score of −3.36 kcal mol^{-1} owing to the creation of hydrogen bonds between hydroxyl group and Lys 244 (2.24 Å). Moreover, it formed salt bridge between the carboxylate anion and Lys 342 (2.95 Å) (Fig. 7i and j). On the other hand, dexamethasone exhibited a g-score of −4.16 kcal mol^{-1} *via* formation of five hydrogen bond interactions: hydroxyl (17)-O group with Lys 52, carbonyl (3) group with Gln 53, both O- and H- of hydroxyl (21) group with Leu 251 and hydroxyl (11)-H group with Glu 341 (Fig. 7 k and l)

Regarding docking with the Voltage Gated Sodium Channel (VGSC), ursolic acid and lidocaine were docked into the centre of the VGSC Nav 1.4-1 channel lumen (Fig. 7m and n), where had a g-score of = −5.59 kcal mol^{-1}, superior to that of lidocaine (−4.077 kcal mol^{-1}) (Table S7†). UA made two H-bonds with Gln 405 (1.94 Å) and Lys 1244 (1.72 Å) (Fig. 7o and p), while lidocaine had only H-bond between its carbonyl group and Gly 1245 (1.87 Å), a hydrophobic interaction *via* the phenyl moiety and Tyr 407 as well as a salt bridge *via* the quaternary nitrogen cation with Asp 1248 and Asp 1539 (Fig. 7q and r).

Docking against matrix metalloproteinase-9 (MMP-9)

The co-crystalized ligand (ID: N73) had a g-score of – 6.30 kcal-mol^{-1} when interacted with the MMP-9 crystal structure (PDB: 4XCT), making hydrogen-bonding interactions with Leu 188 and Ala 189, a Pi–Pi stacking interaction with His 226, a Pi-cation and a metal coordination bond with Zn 302 (Fig. 7s and t, Table S9†). On the other hand, UA interacted efficiently with a g-score = −3.00 kcal mol^{-1} demonstrating hydrogen bonding between Gly 186 and carboxylate anion. It also showed a metal coordination connection between Zn 302 and the hydroxyl group (Fig. 7u and v).

Relative mRNA gene expression

The results of investigating the fold change in relative mRNA gene expression levels revealed a marked upregulation in *TNF-α*, *IL-1β*, *IL-6*, NF-κB and downregulation in *TGF-β* expression levels in the non-treated OA group, compared to the normal group. These levels were markedly reversed in both treatment groups (UA-emulgel and Algason®) with a superior potency of UA-emulgel over Algason. Moreover, the results also showed a distinct upregulation of relative gene expression levels of *COX-II*

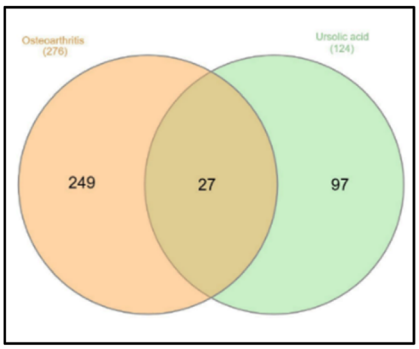

a

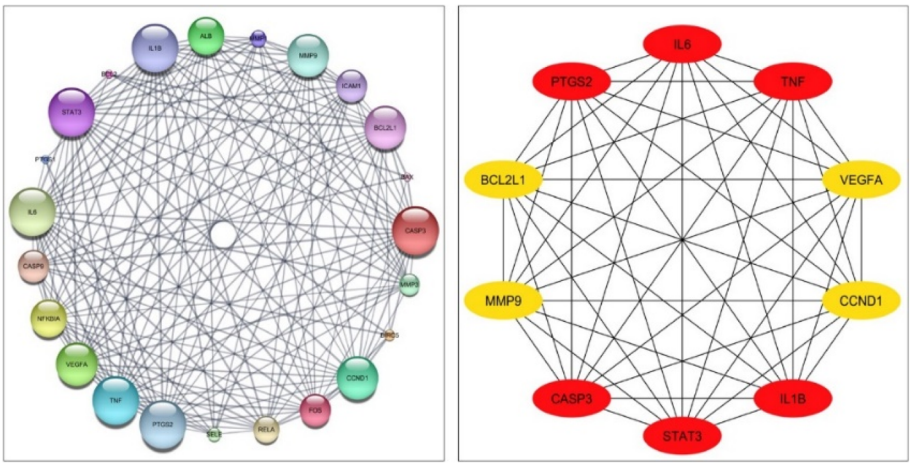

b c

Fig. 6 (a) Venn diagram for the integrated analysis of the related targets of ursolic acid and osteoarthritis, (b) network nodes represent suggested protein targets, and the edges represent protein–protein interactions. The size of nodes signifies the connectivity of each protein, the higher the node size the higher its connectivity to other nodes, (c) the top 10 hub genes: the darker the color, the higher the score and the stronger the connection.

Table 1 Topological parameters of top 10 hub genes with bone tissue expression score

No.	Name	Target	Degree	Betweenness	Closeness	Tissue/bone
1	Interleukin-1 beta	IL-1β	19	0.0303	0.7778	3.3931
2	Signal transducer and activator of transcription 3	STAT3	19	0.0417	0.7544	2.8606
3	Caspase-3	CASP3	19	0.0540	0.7135	3.0570
4	Prostaglandin G/H synthase 2	PTGS2	19	0.0303	0.7778	2.7916
5	Interleukin-6	IL-6	19	0.0303	0.7778	3.5353
6	Tumor necrosis factor	TNF-α	19	0.0303	0.7778	3.4473
7	G1/S-specific cyclin-D1	CCND1	18	0.0376	0.7582	3.3358
8	Bcl-2-like protein 1	BCL2L1	18	0.0467	0.7255	2.4851
9	Matrix metalloproteinase-9	MMP-9	18	0.0108	0.8497	3.1581
10	Vascular endothelial growth factor A	VEGFA	18	0.0108	0.8497	3.3446

MMP-9 and a downregulation of relative gene expression level of TIMP-1, which was reversed in both UA-emulgel and Algason® groups with a superior potency of UA-emulgel (Fig. 8a). Furthermore, the results also revealed a decrease in the ratio of *MMP-9*/*TIMP-1* ratio, which expresses the degree of protection against progressive cartilage damage, in both UA-emulgel and Algason® groups with a superior potency of UA-emulgel (Fig. 8 b).

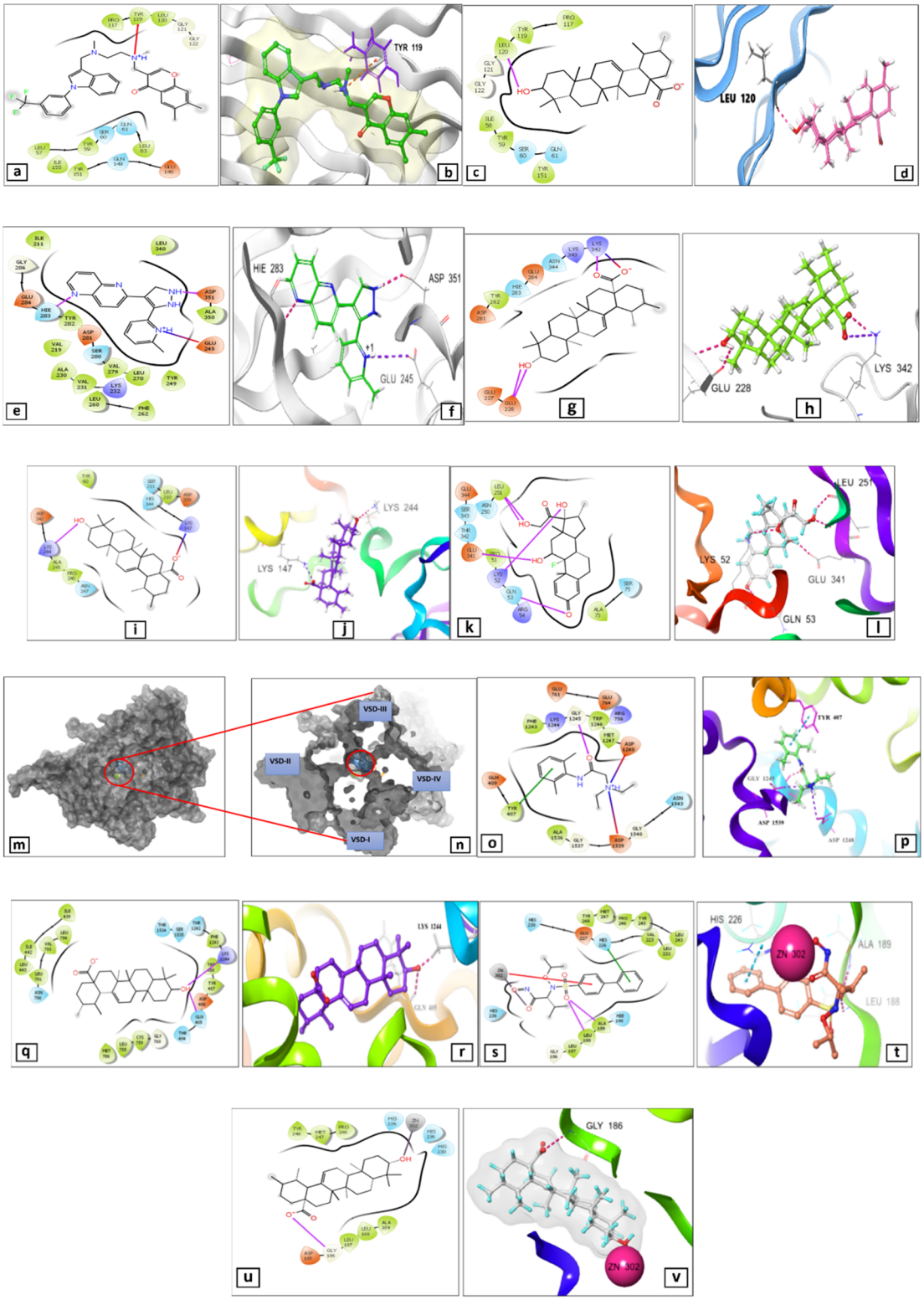

Fig. 7 2D & 3D views (a) & (b) of the ligand 307 re-docked in TNF-α active site, 2D & 3D views (c) & (d) of UA docked in TNF-α active site, 2D & 3D views (e) & (f) of naphthyridine re-docked in TGF-βR1 active site, 2D & 3D views (g) & (h) of ursolic acid docked in TGF-βR1 active site, 2D & 3D views (i) & (j) of UA docked in NF-κB active site, 2D & 3D views (k) & (l) of dexamethasone docked in NF-κB active site, top view (m) & (n) of 3D structure Nav 1.4-β 1 complex consisting of four VSD and Nav 1.4 pore presented in red circle, 2D & 3D views (o) & (p) of ursolic acid docked in Nav 1.4-β1 channel, 2D & 3D views (q) & (r) of Lidocaine docked in Nav 1.4-β1 channel, 2D & 3D views (s) & (t) of co-crystallized ligand (ID: N73) in MMP-9 active site, 2D & 3D views (u) & (v) of UA docked in MMP-9 active site.

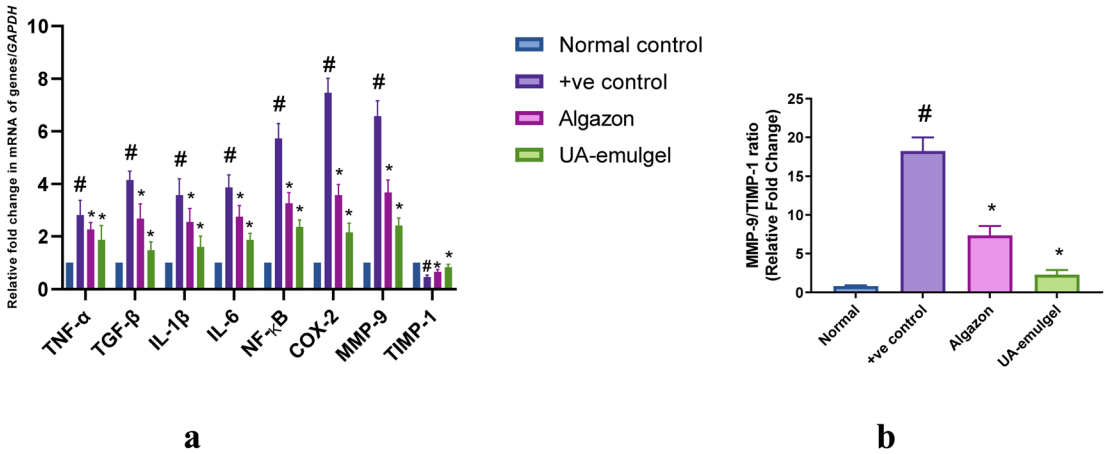

Fig. 8 (a) Gene expression levels using quantitative RT-PCR. Data represent fold change relative to the normal control group. The relative fold change of mRNA was assessed using the $2^{-\Delta\Delta Ct}$ method and normalized to the house keeping gene *GAPDH*. Bars represent mean ± SD. Significant difference between groups is analysed by a one-way ANOVA test, where: $*p < 0.05$ compared with those of the non-treated OA group on the respective day and $\#p < 0.05$ compared with those of the normal control group, (b) MMP-9/TIMP-1 ratios of different OA treatment groups.

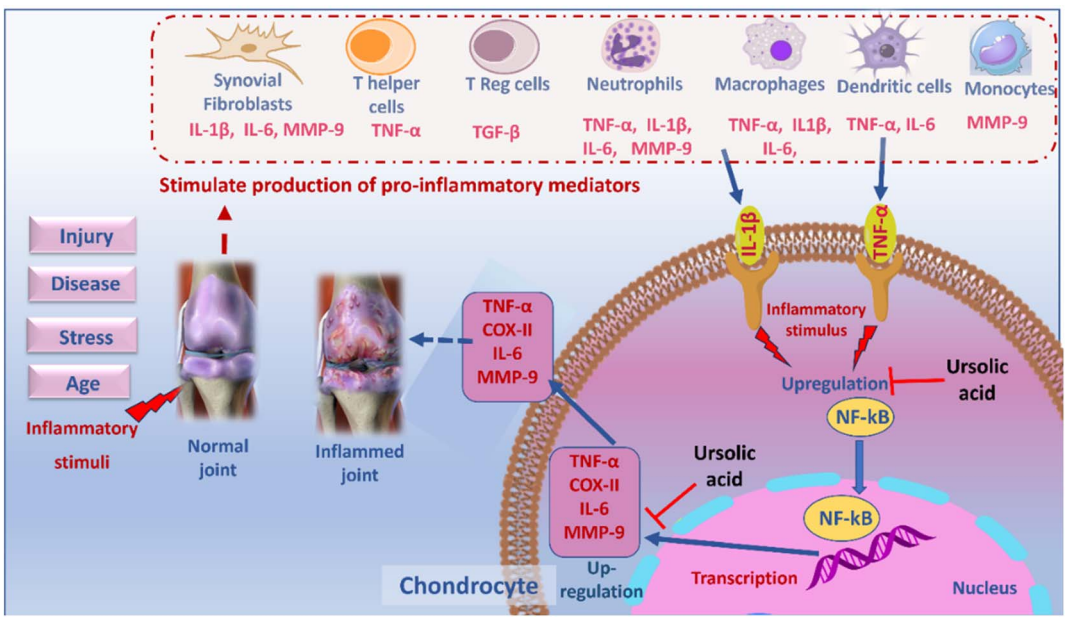

Fig. 9 Proposed mechanism of ursolic acid for management of osteoarthritis.

Discussion

Recently, there has been a growing interest in natural products to replace synthetic ones for the management of chronic diseases.[53,54] The current study assessed the efficacy of topical application of UA in the management of CIA-induced osteoarthritis in early stages. The work started with investigating the chemical composition of the *n*-hexane fraction from *Ocimum forskolei via* LC-HR-MS metabolic profiling, where a total of 19 phytoconstituents belonging to different classes were dereplicated. Among them, UA was the major compound detected in the LC-HR-MS, and it was also heavily precipitated in the total fraction of *n*-hexane. This was followed by its separation by chromatographic techniques and identification *via* NMR. Ursolic acid is reported to inhibit Zymosan-induced acute inflammation and improved symptoms of rheumatoid arthritis in rats by attenuation of pro-inflammatory cytokines.[55] Though the anti-inflammatory potential of UA is verified, a little research is found on its anti-osteoarthritic action, or even the underlying molecular mechanisms. The main obstacle of UA is the poor aqueous solubility and extensive first pass metabolism, making the localized topical delivery systems highly suggested.[18] In addition, the sustained release profile of UA is beneficial not only for the immediate relief of pain and oedema

but also for protecting the cartilage from harmful effects of inflammatory cytokines and diminishing the levels of destructive metalloproteinases.[18]

Accordingly, UA was formulated as emulgel, as emulgels are known as efficiently delivered topical formulations and are comparatively more stable than ointments which experience rancidity, creams that show phase inversion (breaking) or even powders which are hygroscopic.[56] Moreover, emulgels are easily prepared, cost-effective and efficient due to having a large network of gel with perfect drug loading characteristics.[57] In addition, the presence of phospholipids and non-ionic surfactants in the emulgel can act as penetration enhancers.[58] Besides, the emulgel with the highest swelling index attain the highest viscosity and bioadhesion which are preliminary indicators for high stability and spread ability.[59]

The SEM results of the formed emulgel showed unique spherical globules with smooth surfaces generated by the high lecithin/chitosan concentration that enhanced their physical stability.[60] Interestingly, a core/shell structure formed by the action of high viscosity where the more viscous phase (lecithin) formed the core, and the less viscous (chitosan) formed the shell, is recently regarded as one of the most significant breakthroughs in the area of emulsion formation. The core/shell structure significantly affects the dual drug release profile and greatly reduces the direct contact of bioactive agents in an aqueous core solution with the solvents of a shell, leaving only the core–shell interface for maximum bioactivity.[18]

Joint inflammation is known to be established by crosstalk between 2 main cell types: immune cells and joint resident cells. Among the immune cells, the T-helper cells produce pro-inflammatory cytokines which stimulate resident cells (fibroblasts, osteoblasts, osteoclasts and chondrocytes) to secret additional pro-inflammatory factors.[5] These factors create the main joint pathological events as: Synovitis, cartilage damage, pannus and osteophyte formation.[6] Both the immune and joint-resident cells provide feedback on chondrocytes and stimulate production of more pro-inflammatory mediators, functional deregulation of the chondrocytes and subsequent damage.[7]

These pro-inflammatory mediators include: Interleukin-1 Beta (*IL-1β*), one of the key cytokines in OA which attains the ability to shift balance between synthesis and degradation of the extracellular matrix and can induce other pro-inflammatory cytokines including *IL-6*, matrix metalloproteinases (MMPs) and *TNF-α*.[61] Interleukin-6 (*IL-6*) plays a contributory role to the OA pathogenesis and stimulates osteoclast formation, bone resorption and synovitis.[61] In addition, *TNF-α* actuates the innate immune response, *via* promotion of leukocyte recruitment to injured sites, adherence of circulating phagocytic cells and activation of *NF-κB*, resulting in a reduction of synthesis of collagen II, inhibition of *TGF-β* activation and activation of its own secretion in an autocrine manner.[62] Besides, *COX-II* responsible for the production of PGE2, NO and *MMP-9* is also upregulated.[63] Moreover, the MMPs are a series of proteolytic enzymes (especially *MMP-9* produced by monocytes) that downregulate the ECM synthesis and their biological activities are controlled by *TIMP-1* (tissue inhibitor of metalloproteinase), where the imbalance in *MMPs*/*TIMPs* ratio is critical in the OA progression.[61] NF-κB is one of the inflammatory cytokine-induced transcription factors that regulate the expression of iNOS, COX-II, TNF-α, IL-6, MMPs and other cytokines.[64] Normally, NF-κB is present in the cytoplasm in an inactive form which is activated by *IL-1β*, then translocated to the nucleus to trigger the expression of other inflammation-related genes.[61] On the other hand, *TGF-β* is considered a potent anti-inflammatory and immunosuppressive cytokine which opposes the activities of *TNF-α*, promotes downregulation of inflammatory cells and induces generation of T-regulatory cells. Worth mentioning, *TGF-β* upregulates *IL-6* levels, but in the same time it weakens its signaling in chondrocytes *via* down regulation of the *IL-6* receptors.[19] Accordingly, reversing the activity of NF-κB and other aforementioned inflammatory mediators may act as a therapeutic strategy in OA.

Back to the current study, joint inflammation was induced using the CIA-induced mono-arthritis OA model, where UA showed a fast anti-edemic and analgesic action with a significant reversal of disability and mechanical hypersensitivity, accompanied by recovery of hind limb functionality. Additionally, as reported that acute mono-arthritis activates the neurohypophysial system, the local anaesthetic (nerve blockade) potential of UA-emulgel was investigated directly on the sciatic nerve passing through the piriformis muscle and extending down the hind paw, to measure the nerve impulse conduction.[26]

The network strategy in the recent work is built on the "disease-gene-target-pathway-drug" interaction network, that characterizes the impact of drug on the disease network (targets/pathways).[65] The PPI network analysis predicted that 10 targets including *IL-1β*, STAT3, CASP3, PTGS2, *IL-6*, *TNF-α*, CCND1, BCL2L1, *MMP-9*, and VEGFA were the key targets of UA for the treatment of inflammation. Among these key targets in the network, *TNF- α* and *IL-1β* are responsible for the activation of the *NF-κB* pathway by the production of pro-inflammatory stimuli. Upregulation of the *NF-κB* pathway can lead to excessive release of inflammatory cytokines, such as *TNF-α*, *IL-6*, *COX-II* and *MMP-9*.[66] These results afforded preliminary evidence for the pharmacological mechanism that triggers the therapeutic effect of UA on inflammation and cartilage degradation.[67] Accordingly, inflammatory cytokines that were released by these pathways, including *TNF-α*, *IL-6*, *IL-1β*, *MMP-9* and NF-κB, were selected to verify the results of the network pharmacology analyses.

These findings were accomplished by docking studies which showed a strong binding of UA with *TNF-α*, *TGF-β*, *NF-κB*, *MMP-9* as well as the voltage-gated sodium channel, all which ascertained the anti-inflammatory effects of UA and its potential role protecting cartilage degradation and ECM damage as well as analgesic and local anaesthetic properties which collectively aid pain relief and fast healing.[68]

For further confirmation of results, the mRNA gene analyses revealed the upregulation of *TNF-α*, *COX-II*, *IL-6*, *IL-1β*, *MMP-9* and NF-κB pathway, with a significant upregulation of *TIMP-1* and *TGF-β* (Fig. 9). These results are consistent with previous studies, is that UA attenuated the production of the pro-inflammatory cytokines and MMPs.[1] Additionally, UA could attenuate levels of gene expression of NF-κB which attains

a critical role in progression of OA, and could elevate levels of *TGF-β* and *TIMP-1* which collectively promote cartilage repair and chondroprotection.[69,70] The ratio of *MMP-9*/*TIMP-1* was highly elevated in the non-treated OA group (16.25 fold change), reduced in the Algason® group (6 fold change) and excellently reduced to 3 fold change in UA-emulgel group which was much near to the normal ratio (about 1), indicating a high degree of protection of UA treatment Future studies will be needed to explore the detailed mechanism of action of the tested biomarkers in the long-term therapy of OA.

Conclusion and future perspectives

The present study presents an evidence that the topical application of UA-emulgel in CIA-induced model of OA attains a potent analgesic, anti-inflammatory, local anaesthetic and chondroprotective effects. Ursolic acid, among 19 compounds dereplicated from the *n*-hexane fraction of *Ocimum forskolei*, not only can attenuate production of inflammatory cytokines, oxidative and degenerative enzymes, but also mitigates symptoms of OA including spontaneous pain, mechanical allodynia and paw oedema in established *in vivo* acute osteoarthritis model. Owed to multi-target efficacy, wide therapeutic potentials, reported safety, natural abundance and inexpensiveness, we speculate UA to be a good starting point for a herbal-based natural remedy for OA. Ursolic acid offers a strong basis for future long-term animal studies as well as clinical trials, which widely opens the gate for UA to occupy a crucial role in, management, treatment and inhibiting progression of OA.

Author contributions

Conceptualization; E. M. Z., data curation; E. M. Z., M. E., formal analysis; M. H., S. A. M., investigation; E. M. Z., U. R. A., methodology; E. M. Z., S. A. M., project administration; E. M. Z., resources; M. M. E., S. A. M., software; M. H., M. M. E., supervision; M. E., S. Y. D., M. A. F., M. S. K., validation and visualization; E. M. Z., roles/writing – original draft; E. M. Z., S. A. M., writing – review & editing; E. M. Z., U. R. A.

Conflicts of interest

The authors say they have no competing interests.

Acknowledgements

The authors extend their appreciation to Deraya University for supporting this work.

References

1 C. Wang, Y. Gao, Z. Zhang, C. Chen, Q. Chi, K. Xu and L. Yang, Ursolic acid protects chondrocytes, exhibits anti-inflammatory properties *via* regulation of the NF-κB/NLRP3 inflammasome pathway and ameliorates osteoarthritis, *Biomed. Pharmacother.*, 2020, **130**, 110568.
2 T.-M. Chen, Y.-H. Chen, H. S. Sun and S.-J. Tsai, Fibroblast growth factors: Potential novel targets for regenerative therapy of osteoarthritis, *Chin. J. Physiol.*, 2019, **62**, 2.
3 L. Zhang, X. Shi, Z. Huang, J. Mao, W. Mei, L. Ding, L. Zhang, R. Xing and P. Wang, Network Pharmacology Approach to Uncover the Mechanism Governing the Effect of Radix Achyranthis Bidentatae on Osteoarthritis, *BMC Complementary Med. Ther.*, 2020, **20**, 121.
4 C. C. Huang, C. H. Chiou, S. C. Liu, S. L. Hu, C. M. Su, C. H. Tsai and C. H. Tang, Melatonin attenuates TNF-α and IL-1β expression in synovial fibroblasts and diminishes cartilage degradation: implications for the treatment of rheumatoid arthritis, *J. Pineal Res.*, 2019, **66**, e12560.
5 E. M. Zahran, N. M. R. Abdel-Maqsoud, O. Y. Tammam, I. M. Abdel-Rahman, M. A. Elrehany, H. T. Bakhsh, F. H. Altemani, N. A. Algehainy, M. A. Alzubaidi and U. R. J. A. Abdelmohsen, Scabicidal Potential of Coconut Seed Extract in Rabbits *via* Downregulating Inflammatory/Immune Cross Talk: A Comprehensive Phytochemical/GC-MS and *In Silico* Proof, *Antibiotics*, 2022, **12**, 43.
6 M. V. Risbud and I. M. Shapiro, Role of cytokines in intervertebral disc degeneration: pain and disc content, *Nat. Rev. Rheumatol.*, 2014, **10**, 44–56.
7 I. B. McInnes, C. D. Buckley and J. D. Isaacs, Cytokines in rheumatoid arthritis — shaping the immunological landscape, *Nat. Rev. Rheumatol.*, 2016, **12**, 63–68.
8 A. H. Elmaidomy, N. M. R. Abdel-Maqsoud, O. Y. Tammam, I. M. Abdel-Rahman, M. A. Elrehany, H. T. Bakhsh, F. H. Altemani, N. A. Algehainy, M. A. Alzubaidi, F. Alsenani, A. M. Sayed, U. R. Abdelmohsen and E. M. Zahran, Egyptian mandarin peel oil's anti-scabies potential *via* downregulation-of-inflammatory/immune-cross-talk: GC-MS and PPI network studies, *Sci. Rep.*, 2023, **13**, 14192.
9 E. M. Zahran, R. H. Mohyeldin, F. M. Abd El-Mordy, S. A. Maher, N. M. R. Abdel-Maqsoud, F. H. Altemani, N. A. Algehainy, M. A. Alanazi, M. M. Jalal and M. A. Elrehany, Wound healing potential of Cystoseira/mesenchymal stem cells in immunosuppressed rats supported by overwhelming immuno-inflammatory crosstalk, *PLoS One*, 2024, **19**, e0300543.
10 A. H. Elmaidomy, N. M. R. Abdel-Maqsoud, O. Y. Tammam, I. M. Abdel-Rahman, M. A. Elrehany, H. T. Bakhsh, F. H. Altemani, N. A. Algehainy, M. A. Alzubaidi and F. Alsenani, Egyptian mandarin peel oil's anti-scabies potential *via* downregulation-of-inflammatory/immune-cross-talk: GC-MS and PPI network studies, *Sci. Rep.*, 2023, **13**, 14192.
11 E. M. Zahran, U. R. Abdelmohsen, A. S. Hussein, M. A. Salem, H. E. Khalil, S. Yehia Desoukey, M. A. Fouad and M. S. Kamel, Antiulcer potential and molecular docking of flavonoids from *Ocimum forskolei* Benth., family Lamiaceae, *Nat. Prod. Res.*, 2021, **35**, 1933–1937.
12 E. M. Zahran, U. R. Abdelmohsen, M. M. Shalash, M. A. Salem, H. E. Khalil, S. Y. Desoukey, M. A. Fouad, M. Krischke, M. Mueller and M. S. Kamel, Local

anaesthetic potential, metabolic profiling, molecular docking and *in silico* ADME studies of *Ocimum forskolei*, family Lamiaceae, *Nat. Prod. Res.*, 2021, **35**, 4757–4763.

13 E. M. Zahran, U. R. Abdelmohsen, A. Kolkeila, M. A. Salem, H. E. Khalil, S. Y. Desoukey, M. A. Fouad and M. S. Kamel, Anti-epileptic potential, metabolic profiling and *in silico* studies of the aqueous fraction from *Ocimum menthifolium* benth, family Lamiaceae, *Nat. Prod. Res.*, 2021, **35**, 5972–5976.

14 E. M. Zahran, U. R. Abdelmohsen, A. T. Ayoub, M. A. Salem, H. E. Khalil, S. Y. Desoukey, M. A. Fouad and M. S. Kamel, Metabolic profiling, histopathological anti-ulcer study, molecular docking and molecular dynamics of ursolic acid isolated from *Ocimum forskolei* Benth. (family Lamiaceae), *S. Afr. J. Bot.*, 2020, **131**, 311–319.

15 A. H. Elmaidomy, E. M. Zahran, R. Soltane, A. Alasiri, H. Saber, C. J. Ngwa, G. Pradel, F. Alsenani, A. M. Sayed and U. R. Abdelmohsen, New halogenated compounds from *Halimeda macroloba* seaweed with potential inhibitory activity against malaria, *Molecules*, 2022, **27**, 5617.

16 S. Li, Z. Zhang, L. Wu, X. Zhang, Y. Li and Y. Wang, Understanding ZHENG in traditional Chinese medicine in the context of neuro-endocrine-immune network, *IET Systems Biology*, 2007, **1**, 51–60.

17 E. M. Zahran, U. R. Abdelmohsen, A. Kolkeila, M. A. Salem, H. E. Khalil, S. Y. Desoukey, M. A. Fouad and M. S. Kamel, Anti-epileptic potential, metabolic profiling and *in silico* studies of the aqueous fraction from *Ocimum menthifolium* benth, family Lamiaceae, *Nat. Prod. Res.*, 2021, **35**, 5972–5976.

18 S. A. Mohamad, E. M. Zahran, M. R. Abdel Fadeel, A. Albohy and M. A. Safwat, New Acaciin-Loaded Self-Assembled Nanofibers as M(Pro) Inhibitors Against BCV as a Surrogate Model for SARS-CoV-2, *Int. J. Nanomed.*, 2021, **16**, 1789–1804.

19 S. A. Mohamad, E. M. Zahran, M. R. Abdel Fadeel, A. Albohy and M. A. Safwat, New Acaciin-Loaded Self-Assembled Nanofibers as MPro Inhibitors Against BCV as a Surrogate Model for SARS-CoV-2, *Int. J. Nanomed.*, 2021, **16**, 1789–1804.

20 U. Albus, Guide for the Care and Use of Laboratory Animals (8th edn), *Lab. Anim.*, 2012, 267–268.

21 S. A. Rahman, N. S. Abdelmalak, A. Badawi, T. Elbayoumy, N. Sabry and A. E. Ramly, Formulation of tretinoin-loaded topical proniosomes for treatment of acne: in-vitro characterization, skin irritation test and comparative clinical study, *Drug Delivery*, 2015, **22**, 731–739.

22 R. Radhakrishnan, S. A. Moore and K. A. Sluka, Unilateral carrageenan injection into muscle or joint induces chronic bilateral hyperalgesia in rats, *Pain*, 2003, **104**, 567–577.

23 H. Nishimura, M. Kawasaki, T. Matsuura, H. Suzuki, Y. Motojima, K. Baba, H. Ohnishi, Y. Yamanaka, T. Fujitani and M. Yoshimura, Acute mono-arthritis activates the neurohypophysial system and hypothalamo-pituitary adrenal axis in rats, *Front. Endocrinol.*, 2020, **11**, 43.

24 J.-H. Kao, S.-H. Lin, C.-F. Lai, Y.-C. Lin, Z.-L. Kong and C.-S. Wong, Shea nut oil triterpene concentrate attenuates knee osteoarthritis development in rats: Evidence from knee joint histology, *PLoS One*, 2016, **11**, e0162022.

25 J. R. Deuis, L. S. Dvorakova and I. Vetter, Methods Used to Evaluate Pain Behaviors in Rodents, *Front. Mol. Neurosci.*, 2017, **10**, 1–17.

26 J. Sagen, D. A. Castellanos and A. T. Hama, Antinociceptive effects of topical mepivacaine in a rat model of HIV-associated peripheral neuropathic pain, *J. Pain Res.*, 2016, **9**, 361.

27 J. Ru, P. Li, J. Wang, W. Zhou, B. Li, C. Huang, P. Li, Z. Guo, W. Tao, Y. Yang, X. Xu, Y. Li, Y. Wang and L. Yang, TCMSP: a database of systems pharmacology for drug discovery from herbal medicines, *J. Cheminf.*, 2014, **6**, 13.

28 P. Shannon, A. Markiel, O. Ozier, N. S. Baliga, J. T. Wang, D. Ramage, N. Amin, B. Schwikowski and T. Ideker, Cytoscape: a software environment for integrated models of biomolecular interaction networks, *Genome Res.*, 2003, **13**, 2498–2504.

29 F. Prieto-Martínez, M. Arciniega and J. Medina-Franco, Molecular docking: current advances and challenges, *TIP, Rev. Espec. Cienc. Quim.-Biol.*, 2018, 21.

30 F. Gellibert, J. Woolven, M. H. Fouchet, N. Mathews, H. Goodland, V. Lovegrove, A. Laroze, V. L. Nguyen, S. Sautet, R. Wang, C. Janson, W. Smith, G. Krysa, V. Boullay, A. C. De Gouville, S. Huet and D. Hartley, Identification of 1,5-naphthyridine derivatives as a novel series of potent and selective TGF-beta type I receptor inhibitors, *J. Med. Chem.*, 2004, **47**, 4494–4506.

31 E. Nuti, A. R. Cantelmo, C. Gallo, A. Bruno, B. Bassani, C. Camodeca, T. Tuccinardi, L. Vera, E. Orlandini and S. Nencetti, N-O-Isopropyl Sulfonamido-Based Hydroxamates as Matrix Metalloproteinase Inhibitors: Hit Selection and *in Vivo* Antiangiogenic Activity, *J. Med. Chem.*, 2015, **58**, 7224–7240.

32 E. Brzustewicz and E. Bryl, The role of cytokines in the pathogenesis of rheumatoid arthritis – Practical and potential application of cytokines as biomarkers and targets of personalized therapy, *Cytokine*, 2015, **76**, 527–536.

33 A. Yilmaz, H. I. Onen, E. Alp and S. Menevse, *Polymerase Chain Reaction*, 2012, pp. 229–254, DOI: **10.5772/37356**.

34 N. Babu, Therapeutics potential and pharmacological properties of *Leucas indica*: a review, *The Pharma Innovation Journal*, 2018, **7**(7), 564–568.

35 N. Chirikova, D. Olennikov and A. Rokhin, Organic acids from medicinal plants. 4. Scutellaria baicalensis, *Chem. Nat. Compd.*, 2008, **44**, 84–86.

36 D.-M.-C. Nguyen, D.-J. Seo, K.-Y. Kim, R.-D. Park, D.-H. Kim, Y.-S. Han, T.-H. Kim and W.-J. Jung, Nematicidal activity of 3,4-dihydroxybenzoic acid purified from *Terminalia nigrovenulosa* bark against *Meloidogyne incognita*, *Microb. Pathog.*, 2013, **59–60**, 52–59.

37 A. Suzuki, O. Shirota, K. Mori, S. Sekita, H. Fuchino, A. Takano and M. Kuroyanagi, Leishmanicidal active constituents from Nepalese medicinal plant Tulsi (*Ocimum sanctum* L.), *Chem. Pharm. Bull.*, 2009, **57**, 245–251.

38 E. M. Zahran, U. R. Abdelmohsen, H. E. Khalil, S. Y. Desoukey, M. A. Fouad and M. S. Kamel, Diversity,

phytochemical and medicinal potential of the genus Ocimum L. (Lamiaceae), *Phytochem. Rev.*, 2020, **19**, 907–953.

39 N. Z. Z. Mamadalieva, D. K. K. Akramov, L. A. A. Wessjohann, H. Hussain, C. Long, K. S. S. Tojibaev, E. Alshammari, M. L. L. Ashour and M. Wink, The Genus Lagochilus (Lamiaceae): A Review of Its Diversity, Ethnobotany, Phytochemistry, and Pharmacology, *Plants*, 2021, **10**, 132.

40 A. Karioti, T. Milošević-Ifantis, N. Pachopos, N. Niryiannaki, D. Hadjipavlou-Litina and H. Skaltsa, Antioxidant, anti-inflammatory potential and chemical constituents of Origanum dubium Boiss., growing wild in Cyprus, *J. Enzyme Inhib. Med. Chem.*, 2015, **30**, 38–43.

41 L. Xiao-zhen, Y. Yong-ming and C. Yong-xian, Compounds from *Clerodendranthus spicatus*, *Nat. Prod. Res. Dev.*, 2017, **29**, 183–189.

42 A. Hadipanah, M. Gheisari and A. Armin, Chemical analysis and identification of the components of Black Seed and Thyme cultivated in Iran, *Sci. Agric.*, 2013, **4**, 55–57.

43 H. Kühn, R. Wiesner, L. Alder and T. Schewe, Occurrence of free and esterified lipoxygenase products in leaves of *Glechoma hederacea* L. and other Labiatae, *Nat. Prod. Res. Dev.*, 1989, **186**, 155–162.

44 C. Garcia, C. Teodósio, C. Oliveira, C. Oliveira, A. Díaz-Lanza, C. Reis, N. Duarte and P. Rijo, Naturally Occurring Plectranthus-derived Diterpenes with Antitumoral Activities, *Curr. Pharm. Des.*, 2018, **24**, 4207–4236.

45 R. Pereda-Miranda, L. Hernández, M. J. Villavicencio, M. Novelo, P. Ibarra, H. Chai and J. M. Pezzuto, Structure and Stereochemistry of Pectinolides A-C, Novel Antimicrobial and Cytotoxic 5,6-Dihydro-α-pyrones from *Hyptis pectinata*, *J. Nat. Prod.*, 1993, **56**, 583–593.

46 A. El-Lakany, New Rearranged Abietane Diterpenoids from the Roots of *Salvia aegyptiaca* L. Growing in Egypt, *Nat. Prod. Sci.*, 2003, **9**, 220–222.

47 B. Abegaz and H. Kinfe, Naturally Occurring Homoisoflavonoids: Phytochemistry, Biological Activities, and Synthesis (Part II), *Nat. Prod. Commun.*, 2019, **14**, 1934578X1984581.

48 S. N. Ebrahimi, S. Zimmermann, J. Zaugg, M. Smiesko, R. Brun and M. Hamburger, Abietane diterpenoids from *Salvia sahendica*–antiprotozoal activity and determination of their absolute configurations, *Planta Med.*, 2013, **29**, 150–156.

49 M. Villalva, S. Santoyo, L. Salas-Pérez, M. d. l. N. Siles-Sánchez, M. Rodríguez García-Risco, T. Fornari, G. Reglero and L. Jaime, Sustainable Extraction Techniques for Obtaining Antioxidant and Anti-Inflammatory Compounds from the Lamiaceae and Asteraceae Species, *Foods*, 2021, **10**, 2067.

50 Y. Yin, K. Zhang, L. Wei, D. Chen, Q. Chen, M. Jiao, X. Li, J. Huang, Z. Gong and N. Kang, The Molecular Mechanism of Antioxidation of Huolisu Oral Liquid Based on Serum Analysis and Network Analysis, *Front. Pharmacol.*, 2021, **12**, 1–20.

51 Y. Tang, M. Wang, X. Le, J. Meng, L. Huang, P. Yu, J. Chen and P. Wu, Antioxidant and Cardioprotective Effects of Danshensu (3-(3,4-Dihydroxyphenyl)-2-Hydroxy-Propanoic Acid from *Salvia miltiorrhiza*) on Isoproterenol-Induced Myocardial Hypertrophy in Rats, *Phytomedicine*, 2011, **18**(12), 1024–1030.

52 M. Silva, I. Vieira, F. Mendes, I. Albuquerque, R. Santos, F. Silva and S. Morais, Variation of Ursolic Acid Content in Eight Ocimum Species from Northeastern Brazil, *Molecules*, 2008, **13**, 2482–2487.

53 E. M. Zahran, A. M. Sayed, R. Alaaeldin, M. A. Elrehany, A. R. Khattab and U. R. Abdelmohsen, Bioactives and functional food ingredients with promising potential for the management of cerebral and myocardial ischemia: a comprehensive mechanistic review, *Food Funct.*, 2022, **13**, 6859–6874.

54 E. M. Zahran, R. H. Mohyeldin, F. M. A. El-Mordy, S. A. Maher, O. Y. Tammam, E. A. Saber, F. H. Altemani, N. A. Algehainy, M. A. Alanazi and M. D. Jalal, Wound Restorative Power of Halimeda macroloba/Mesenchymal Stem Cells in Immunocompromised Rats *via* Downregulating Inflammatory/Immune Cross Talk, *Mar. Drugs*, 2023, **21**, 336.

55 S.-y. Baek, J. Lee, D.-g. Lee, M.-k. Park, J. Lee, S.-k. Kwok, M.-l. Cho and S.-h. Park, Ursolic acid ameliorates autoimmune arthritis *via* suppression of Th17 and B cell differentiation, *Acta Pharmacol. Sin.*, 2014, **35**, 1177–1187.

56 D. Bhowmik, Recent advances in novel topical drug delivery system, *Pharma Innovation*, 2012, **1**, 12–31.

57 E. Raj and S. Balakrishnan, Short Review-Emulgel, *J. Compr. Pharm.*, 2016, **3**, 208–224.

58 C. T. Ueda, V. P. Shah, K. Derdzinski, G. Ewing, G. Flynn, H. Maibach, M. Marques, H. Rytting, S. Shaw and K. Thakker, *Pharmacopeial Forum*, 2009, **35**, 750–764.

59 A. Panwar, N. Upadhyay, M. Bairagi, S. Gujar, G. Darwhekar and D. Jain, Emulgel: a review, *Asian J. Pharm. Life Sci.*, 2011, **2231**, 4423.

60 R. Mikula and V. Munoz, Characterization of emulsions and suspensions in the petroleum industry using cryo-SEM and CLSM, *Colloids Surf., A*, 2000, **174**, 23–36.

61 G. Livshits and A. Kalinkovich, Hierarchical, imbalanced pro-inflammatory cytokine networks govern the pathogenesis of chronic arthropathies, *Osteoarthritis Cartilage*, 2018, **26**, 7–17.

62 M. Varela, A. Romero, S. Dios, M. van der Vaart, A. Figueras, A. H. Meijer and B. Novoa, Cellular visualization of macrophage pyroptosis and interleukin-1β release in a viral hemorrhagic infection in zebrafish larvae, *J. Virol.*, 2014, **88**, 12026–12040.

63 T. Rathinavel, S. Ammashi and G. Shanmugam, Analgesic and anti-inflammatory potential of Lupeol isolated from Indian traditional medicinal plant *Crateva adansonii* screened through *in vivo* and *in silico* approaches, *J. Genet. Eng. Biotechnol.*, 2021, **19**, 1–14.

64 N. Elmali, I. Esenkaya, A. Harma, K. Ertem, Y. Turkoz and B. Mizrak, Effect of resveratrol in experimental osteoarthritis in rabbits, *Inflammation Res.*, 2005, **54**, 158–162.

65 B. Yang, W. Bao, J. Wang, B. Chen, N. Iwamori, J. Chen and Y. J. Chen, Disease-related compound identification based on deeping learning method, *Sci. Rep.*, 2022, **12**, 20594.
66 T. Al-Warhi, E. M. Zahran, S. Selim, M. M. Al-Sanea, M. M. Ghoneim, S. A. Maher, Y. A. Mostafa, F. Alsenani, M. A. Elrehany and M. S. Almuhayawi, Antioxidant and wound healing potential of *Vitis vinifera* seeds supported by phytochemical characterization and docking studies, *Antioxidants*, 2022, **11**, 881.
67 L. He, Y. Pan, J. Yu, B. Wang, G. Dai and X. Ying, Decursin alleviates the aggravation of osteoarthritis *via* inhibiting PI3K-Akt and NF-κB signal pathway, *Int. Immunopharmacol.*, 2021, **97**, 107657.
68 M. M. Richards, J. S. Maxwell, L. Weng, M. G. Angelos and J. Golzarian, Intra-articular treatment of knee osteoarthritis: from anti-inflammatories to products of regenerative medicine, *Phys. Sportsmed.*, 2016, **44**, 101–108.
69 R. Wiegertjes, A. van Caam, H. van Beuningen, M. Koenders, P. van Lent, P. van der Kraan, F. van de Loo and E. Blaney Davidson, TGF-β dampens IL-6 signaling in articular chondrocytes by decreasing IL-6 receptor expression, *Osteoarthr. Cartil.*, 2019, **27**, 1197–1207.
70 R. Khullar, D. Kumar, N. Seth and S. Saini, Formulation and evaluation of mefenamic acid emulgel for topical delivery, *Saudi Pharm. J.*, 2012, **20**, 63–67.